A Microwave Measuring System for Detecting and Localizing Anomalies in Metallic Pipelines

Andrea Cataldo, *Senior Member, IEEE,* Egidio De Benedetto, *Senior Member, IEEE,*
Leopoldo Angrisani, *Fellow, IEEE,* Giuseppe Cannazza, and Emanuele Piuzzi, *Member, IEEE*

***Abstract*—In this work, an innovative system for structural health monitoring of metallic pipes is presented. The proposed system relies on using the pipeline as a waveguide for the propagation of an electromagnetic (EM) signal. Possible anomalies in the pipe provoke the partial reflection of the propagating signal. Differently from previous works, in relation to the proposed application, the EM test signal is injected in the pipeline/waveguide through a coaxial/waveguide transition that is made on the surface of the pipe (rather than on a cross-section as generally done). In practical applications, this strategy would allow to connect more easily to operating, buried pipes.**
Additionally, because reflections caused by anomalies may be difficult to identify with adequate accuracy, the authors have developed a dedicated processing strategy for the analysis of the reflections caused by anomalies. More specifically, by analyzing the measured reflected signal and by correlating it to the ideal reflected signal, it is possible to improve the localization of anomalies along the pipe. The proposed system, along with the processing and operating strategies were validated through full-wave simulations and experimental tests carried out on a steel pipe in presence of intentionally-provoked anomalies.

***Index Terms*—Leak detection, microwave monitoring, microwave reflectometry, microwave measurements, pipelines, reflectograms, structural health monitoring, circular waveguide**

I. Introduction

PIPELINES are the safest and most economic means to transport fluids [1]. Monitoring their integrity is therefore crucial to limit financial losses, and also for safety reasons and for avoiding environmental pollution [2]. When failures (or incipient failures) are not detected in time, it could result in major breakdowns of the pipeline infrastructure [3].
At the state of the art, there are a number of methods for structural health monitoring of pipelines: magnetostrictive sensors [4], back-scattering sensors [5], acoustic emission sensors [6], and so on. In [7], a comprehensive review of the state-of-the-art methods for structural monitoring of buried pipes is presented. The most popular systems are based on acoustic methods [8]; in particular, guided wave inspection systems are largely used to detect damage in pipes [9]–[13]. These systems, which are based on the use of low-frequency acoustic waves (in the order of 10 kHz), rely on positioning rings of transducers (generally, piezoelectric) approximately a quarter wavelength apart along the pipe [10]. In these cases, the echo signal is measured to detect defects or other anomalies that compromise the integrity of the pipe.

Starting from the general principle of these type of systems (e.g., propagation of waves and measurement of the echo signal), several works in the literature have addressed the possibility of using high-frequency electromagnetic (EM) signal for structural monitoring of underground metallic pipes. In particular, the metallic pipe is used as a circular waveguide for propagating the EM signal. For example, in [14], a numerical analysis was presented regarding the nondestructive test of wall thinning in spiral-welded pipes. The analysis was based on the variation of the peaks of the reflection and of transmission scattering parameter in frequency domain. In [15], a microwave method using the pipe as a waveguide was presented: the measured amplitudes of the microwave signal versus frequency showed that different wall thinning values in the same pipe section led to variations of the resonance frequency. In [16], a quantitative nondestructive testing (NDT) method, based on the analysis of the reflection and of the transmission scattering parameters, to detect both wall thinning and biofilm inside a metal pipe was presented and validated through laboratory tests. Also, in [17], a NDT method using microwave guided wave was employed to detect semi-circumferential cracks in piping system, resorting to the estimation of the time of flight of the injected EM signal.
However, in these works, the test signal is injected through a cross-section of the pipe. Hence, when a pipe is installed, it becomes impractical to propagate the EM signal by connecting to a waveguide port.

To circumvent this issue, in this work, the EM test signal is fed through a coaxial to waveguide transition made on the wall of the pipe, as shown in Fig. 1 [18]. This strategy removes the connection limitation, and makes the proposed system potentially viable for on-site localization of anomalies in pipes; in fact, in practical applications, this strategy would allow to connect more easily to operating, buried pipes.
Additionally, because reflections caused by anomalies may be difficult to identify directly from the reflected EM signal, the authors developed and implemented a dedicated processing strategy for the analysis of the reflections caused by anomalies. More specifically, by analyzing the measured reflected signal and by correlating it to the ideal reflected signal, it is possible to improve the localization of anomalies along the pipe. The

A. Cataldo and G. Cannazza are with the Department of Engineering for Innovation - University of Salento, 73100 Lecce, Italy e-mail: andrea.cataldo@unisalento.it, giuseppe.cannazza@unisalento.it.
E. De Benedetto and L. Angrisnani are with with the Department of Information Technology and Electrical Engineering - University of Naples Federico II, 80125 Naples, Italy e-mail: angrisan@unina.it, egidio.debenedetto@unina.it
E. Piuzzi is with the Department of Information Engineering, Electronics and Telecommunications (DIET) Sapienza - University of Rome Via Eudossiana, 00184 Rome - Italy e-mail: emanuele.piuzzi@uniroma1.it.
Manuscript received Month XX, 2020; revised Month XX, 2020.

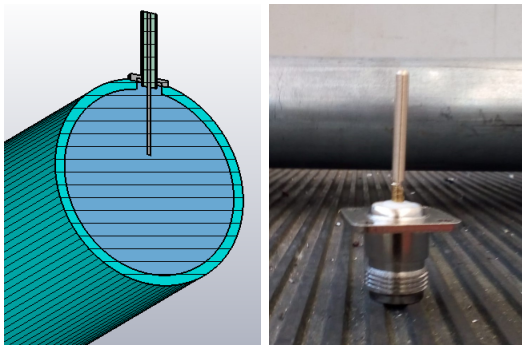

(a) (b)

Fig. 1. Sketch of the perspective cross-section view of the hollow pipe, the particular of the coaxial-to-waveguide transition is also shown (a); picture of the connector used in practice for the transition coaxial-to-waveguide (b).

ideal reflected signal is created analytically, by considering an ideal TE11 mode propagating in a lossless circular waveguide (i.e., the healthy pipe).

Finally, because the microwave signal is injected through the surface of the pipe, clearly it can propagate in two directions. As a result, it is not possible to discriminate from which direction the reflection is coming. To remove this ambiguity, the authors developed an operating strategy that consists in placing two independent and non-interfering coaxial-to-waveguide transition connectors at a distance from each other. In practical applications, when an anomaly is detected from the measurement at one test-point, a separate measurement at a second test-point can be used as a cross-reference to identify the position of the reflection/anomaly.

The proposed system, along with the processing and operating strategies were validated through full-wave simulations and experimental tests carried out on a steel pipe in presence of intentionally-provoked anomalies.

II. Theoretical Background, Processing Strategy, and Preliminary Validation

The proposed system relies on microwave reflectrometry measurements on the pipe. The considered geometry consisted of a steel pipe, considered as a circular waveguide propagating the fundamental TE11 mode. Considering the pipes available for the subsequent experiment, the inner and outer diameters are equal to 54 mm and 60 mm, respectively: these dimensions allow the propagation of the TE11 mode.

As schematized in Fig. 1(a), a section of an RG58 coaxial cable propagates the EM signal up to the pipe. At the pipe wall, at a position $N1$, a coaxial to waveguide transition is created. At the transition, the central conductor of the cable protrudes inside the pipe. To optimize impedance matching, the protrusion depth was optimized through full-wave simulations carried out through CST Microwave Studio. In particular, simulations were carried out considering the actual geometry of the transition (as shown in Fig. 1), an varying the penetration depth was varied. It was observed that the best matching was obtained for a protrusion length of 19 mm: Figure 2 shows the corresponding simulation results. It can be noticed that, in the frequency range of interest (e.g., that of

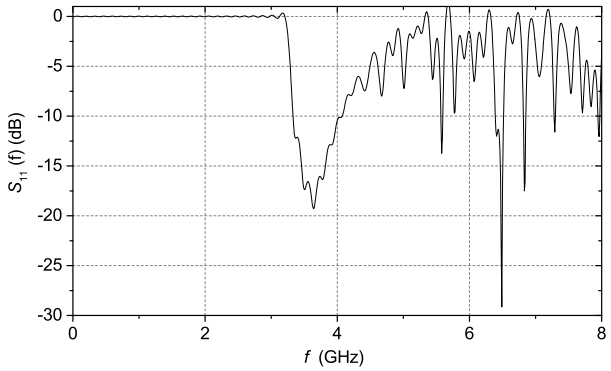

Fig. 2. Simulation results of the return losses at the coaxial-to-waveguide transition for a protrusion length of 19 mm.

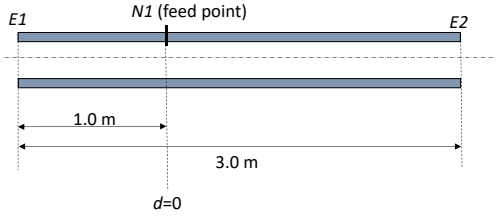

Fig. 3. Sketch of the experimental setup for the preliminary validation of the proposed method and processing strategy. A 3 m-long steel pipe, with a feed point at $N1$ *(dimensions no to scale)*.

TE11 mode propagation, 3.2 - 4.6 GHz), a very good matching is obtained.

A. Reflectometric measuring instrumentation

Because of the necessity to investigate a specific frequency band (3.2 - 4.6 GHz), it was not possible to employ a traditional reflectometer (which, usually, employs a pulse signal or a step-like signal [19], [20]).

For this reason, all the reflectometry measurements were carried out starting from measurement of the reflection scattering parameter, S_{11}, of the structure. Measurements of the S_{11} were carried out through the VNA R&S ZVA50 vector network analyzer. The VNA was calibrated through a short-open-load (SOL) calibration carried out at the N-type connector, by using the Agilent 85032B Type N calibration kit. The calibration was carried out at the end of the coaxial cable. Nevertheless, as detailed in the following, for the localization of the anomalies, the coax-to-waveguide transition is considered: this is identified in correspondence of the first reflection.

B. Processing Strategy

As mentioned in the previous section, reflections caused by anomalies may be difficult to identify directly from the reflected signal. For this reason, a dedicated processing strategy for the analysis of the reflections caused by anomalies was developed. The processing strategy relies on the time-domain correlation between the measured reflected signal, $r(t)$, and the reflected signal that would be expected theoretically if a reflection should happen in the pipe at a distance d from the

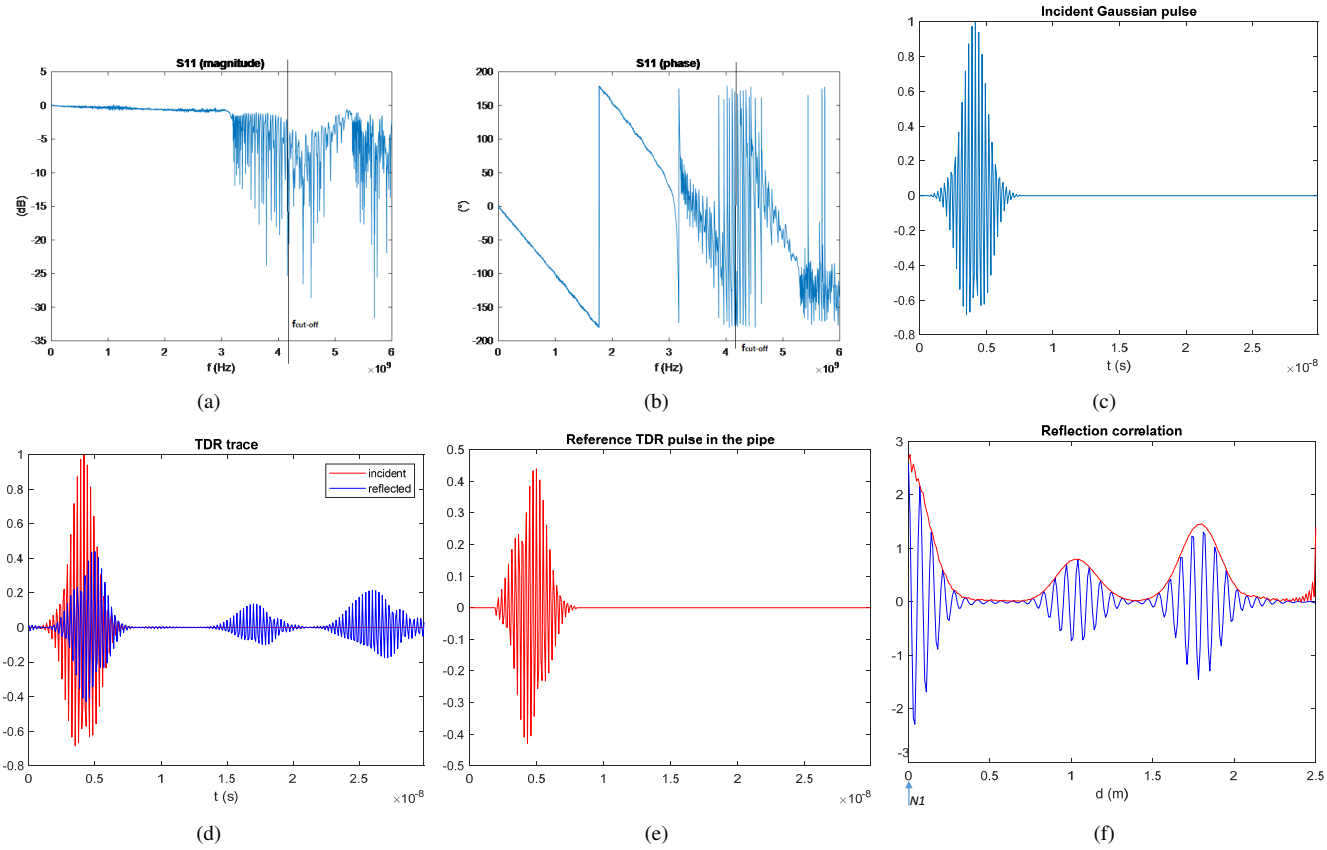

(a) (b) (c) (d) (e) (f)

Fig. 4. Steps of the processing procedure: Measurement of the reflections scattering parameter (a), (b); ideal input signal generated in Matlab (c); incident signal and reflected signal (d); first reflection (e); envelope (f)

transition, $v_{r,ref}(t)$.

In the following, the steps of the processing procedure are described in detail, along with the results obtained by applying the procedure on a 3.0 m-long steel pipe. Figure 3 shows a sketch of the experimental setup. The letters $E1$ and $E2$ indicate the two ends of the pipe. The excitation port, $N1$ was placed at a distance of 1.0 m from $E1$. For the transition, an N-type connector was used, as shown in Fig. 1(b).

The first step of the procedure consists in measuring the reflection scattering parameter, $S_{11}(f)$, in magnitude and phase, as shown in Fig. 4(a) and Fig. 4(b).

Then, a pulse input signal, $i(t)$, is created in Matlab, as shown in Fig. 4(c). This is a Gaussian-modulated sinusoidal pulse, with a frequency band in the 3.2-4.6 GHz range. Considering the diameter of the steel pipe to be used for the experimental validation, this frequency range allows the propagation of the TE11 mode, while undesired higher-order modes are still under cut-off.

Successively, the fast Fourier transform of $i(t)$ is calculated, $I(f)$. Through the inverse fast Fourier transform of the product between $I(f)$ and the measured $S_{11}(f)$, it is possible to calculate the time-domain reflected pulse signal, $r(t)$, shown in Fig. 4(d):

$$r(t) = \mathcal{F}^{-1}\{R(f)\} = \mathcal{F}^{-1}\{I(f)S_{11}(f)\} \tag{1}$$

From $r(t)$, only the first reflection is windowed in, as shown in Fig. 4(e): this corresponds to the coaxial-to-waveguide transition. The resulting signal is then considered as the reference pulse signal that is propagated in the pipe, $v_{ref}(t)$. The next step consists in calculating the theoretical reflection in correspondence of an obstacle at a generic distance d from the test-point. This is calculated through the following equation:

$$V_{r,ref}(f,d) = V_{ref}(f) \cdot exp(-2jk_z(f)d) \tag{2}$$

where $V_{ref}(f) = \mathcal{F}\{v_{ref}(t)\}$; while $k_z(f)$ is the frequency-dependent complex propagation constant.

Assuming a TE11 mode propagating in a circular waveguide, the value of $k_z(f)$ can be evaluated as

$$k_z^2(f) = (2\pi f)^2\mu_0\varepsilon_0 - \left(\frac{1.841}{r}\right)^2, \tag{3}$$

where $\varepsilon_0 = 8.854\times10^{-12}$ F/m is the permittivity of free space; $\mu_0 = 4\pi \times 10^{-7}$ H/m is the permeability of free space; f is the frequency; and r is the radius of the waveguide [21]. It should be noted that, if a liquid fills the pipe, then ε_0 must be multiplied by the complex relative dielectric permittivity of the liquid.

The quantity $V_{ref}(f)$ is then transformed into the TD through the following equation:

$$v_{r,ref}(t,d) = \mathcal{F}^{-1}\{V_{r,ref}(f,d)\} \tag{4}$$

This represents the reflected pulse signal that corresponds to a reflection at a generic distance d from the test point.

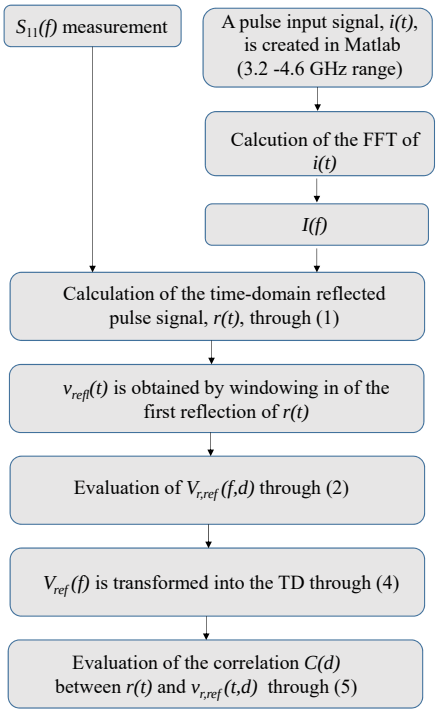

Fig. 5. Flow-chart summarizing the major steps of the processing procedure.

Fig. 6. Picture of the experimental setup for a 6 m-long pipe.

Finally, by varying d, the correlation between the time-domain reflected pulse signal, $r(t)$ and the quantity $v_{r,ref}(t,d)$ is calculated:

$$C(d) = \int_{-\infty}^{\infty} r(t) \cdot v_{r,ref}(t,d)dt \tag{5}$$

The resulting correlation is shown in Fig. 4(f). Finally, the envelope of the correlated signal is calculated: more specifically, it is obtained as the magnitude of the analytical signal evaluated in Matlab through the Hilbert function (red curve of Fig. 4(f)). Higher values of correlation will correspond to the presence of a reflection. In particular, each peak in the correlation envelope corresponds to the location of a possible anomaly. Figure 5 summarizes the major steps of the proposed processing procedure.

C. *Discussion the preliminary results*

Figure 4(f) shows the correlation between the reflected signal and the theoretical reflected signal. With reference to the sketch of Fig. 3, the test signal is fed at the point $N1$. Hence, the input signal travels towards both ends of the pipe: $E1$ (at 1.0 m from $N1$) and $E2$ (at 2.0 m from $N1$). The ends of the pipe can be considered as non-ideal open circuit terminations; therefore, when the incident signal reaches these sections, it is partially reflected.

It should be mentioned that the origin of the abscissa, d = 0 m, corresponds to the position of the feed-point: $N1$ in this case. It can be noticed that the first reflection after the transition occurs at a distance of approximately d = 0.93 m. This corresponds to the reflection caused by the end $E1$ of the pipe. The next major peak of the correlation occurs at approximately d = 1.93 m, and it is related to the reflection caused by the $E2$ end of the pipe.

This preliminary experiment showed that the proposed system can successfully identify the length of the pipe and the position of the ends of the pipe. Basically, in the considered experiment, the ends of the pipe can be considered as anomalies.

III. Description of the Experiments

After the preliminary validation of the system, additional experimental tests were carried out to test the system on longer pipes and to verify its performance in presence of pipe anomalies. To this purpose, experiments were carried out on 6.0 m-long pipes. Figure 6 shows a picture of the setup, while Fig. 7(b) and Fig. 7(d) show the sketches of the setup. Also in these cases, the inner and outer diameters of the pipes were equal to 54 mm and 60 mm.

To assess the response of the measurement system in presence of anomalies in the pipe, measurements were carried out on the empty pipe emulating different types of possible damage:

- healthy pipe condition;
- emulating a thickening of the inner wall of the pipe (wall thickening is, in fact, a typical phenomenon that occurs in pipes);
- same as before, with a different longitudinal extension of the emulated thickening effect;
- making cuts on the pipe (mimicking the cause of pipe leakages).

Finally, measurements were also carried out by filling the pipe with diesel oil, to test the performance of the system in presence of a lossy fluid.

Two different and independent feedpoints, $N1$ and $N2$, were placed as shown in the sketch of Fig. 7. The two feedpoints were used separately and independently for the

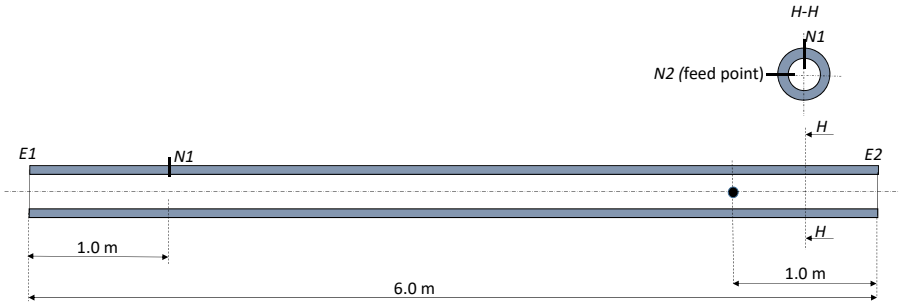

(a)

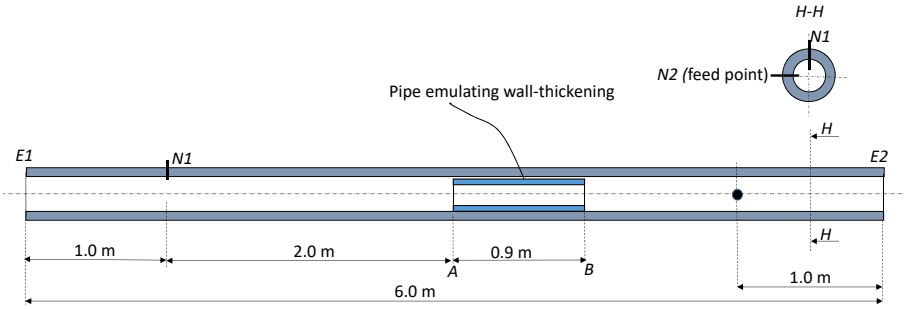

(b)

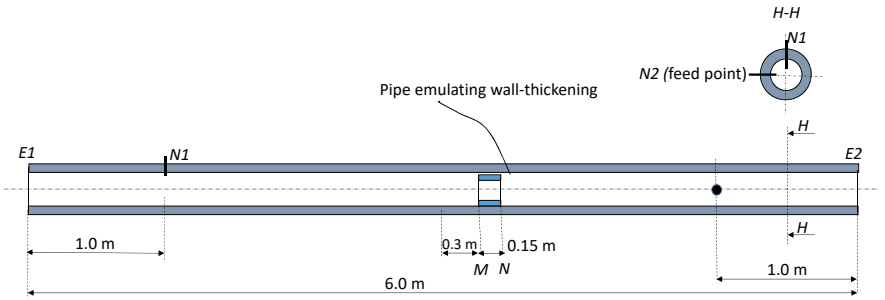

(c)

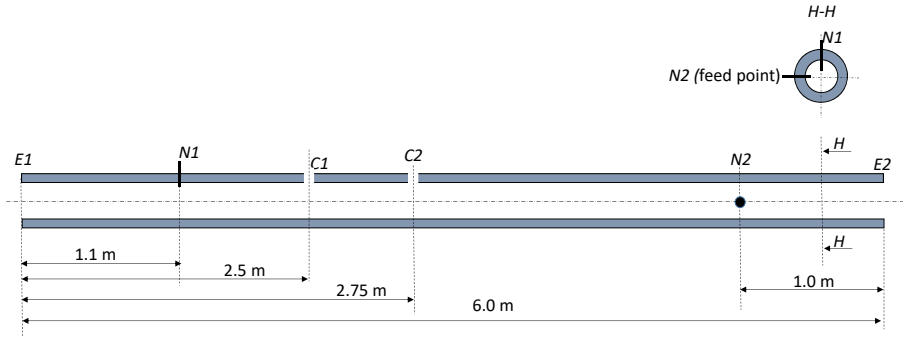

(d)

Fig. 7. Schematization of the 6 m-long pipes: (a) healthy pipe; (b), (c) setup for emulating wall thickening and (d) setup for emulating the response of the system in presence of cuts, $C1$ and $C2$ (*dimensions not to scale*).

reflectometric measurements. More specifically, for this configuration, the two test-points were rotated 90° with respect to each other (hence, they were cross-polarized), as shown in the cross section in the onset of the figure. This allowed exploiting two independent orthogonal TE11 modes. This arrangement ensured that one feed point would only minimally disturb the wave launched from the other port, thus eliminating undesired reflections.

In fact, as mentioned in Section I, because the EM signal is injected through the surface of the pipe, obviously it can propagate in two directions. As a result, it is not possible to discriminate from which direction the reflection is coming. On the other hand, having two feed points available, when an anomaly is detected from the measurement at one port, a separate measurement at the second port can be used as a cross-reference to identify the position of the reflection/anomaly.

The presence of two orthogonal test points also allow to overcome possible problems that might occur when the pipe is filled with a dielectric. In fact, in this case, any discontinuity in the dielectric material may change the polarization of the signal, and this may end up affecting the optimal position of the connector. Including two perpendicular connectors ($N1$ and $N2$), also allows to overcome the aforementioned phenomenon.

IV. Experimental Results

A. Case #1: 6 m-long healthy pipe

Figure 7(a) shows the sketch of the experimental setup. First, measurement was carried out at port $N1$: Fig. 8(a) shows the result of the correlation, which shows the presence of two major peaks. The origin of the distance axis corresponds to the position of $N1$. The first correlation peak corresponds to the pipe end $E1$ which, from the correlation, appears at a distance d_{E1}^{N1}=0.93 m from $N1$. The second reflection occurs at d_{E2}^{N1}= 4.79 m, which corresponds to the distance of the end $E2$ from the feed point $N1$. It appears that there are distinct correlations caused by the reflections at the ends of the pipe.

Measurements were repeated by connecting the VNA to port $N2$. The correlation results are shown in Fig. 8(b). In this case, the origin of the distance axis corresponds to the position of the $N2$ port. Also in this case, two major correlation peaks can be noticed, corresponding to the ends of the pipe. More specifically, the reflection caused by $E1$ occurs at a distance d_{E1}^{N2} = 0.93 m, while the reflection caused by $E2$ occurs at a distance d_{E2}^{N2} = 4.76 m from $N2$.

Results show that, also for the 6 m-long pipe, the proposed system can detect with good accuracy the truncation of the pipe. It is important to notice that the correlations obtained from either the feedpoints are compatible with each other.

B. Case #2: 6 m-long pipe with emulated wall thickening

Wall thickening is a typical anomaly that occurs in pipes. It is caused by accumulation of material that gets stuck in the pipe and accumulates over time. Basically, the wall thickening emulates the presence of a non-conductive material that deposits on the inner surface of the pipe; hence, it creates a reflection that is larger than a thickening of steel. In this

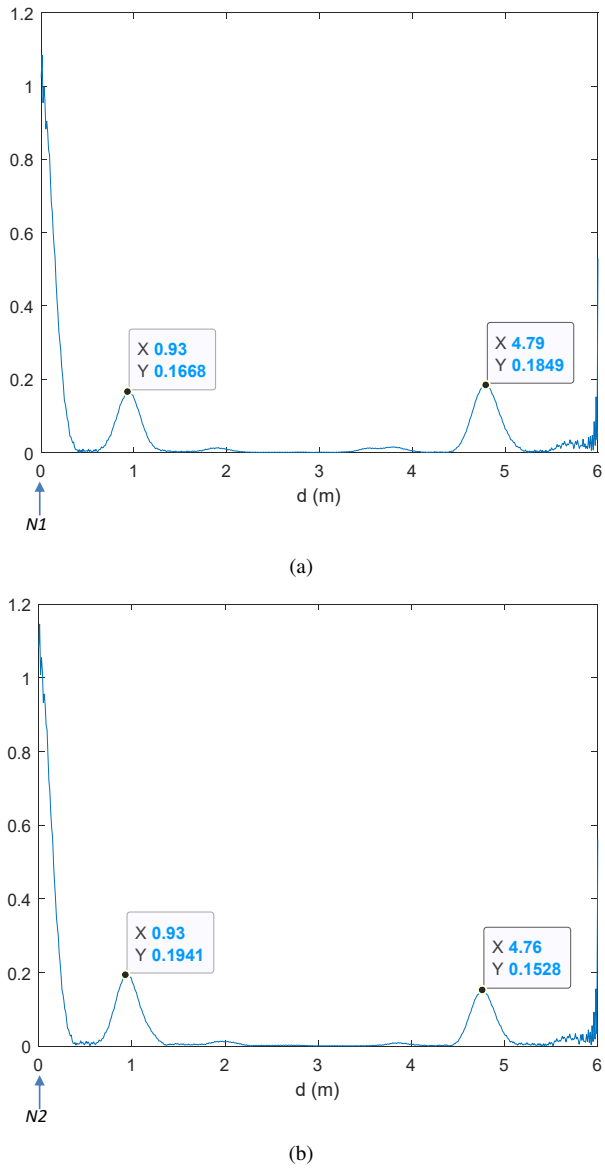

Fig. 8. Measurements on a 6 m-long, empty pipe as schematized in Fig. 7(a). Correlation results obtained through measurements at port $N1$ (a) and at port $N2$ (b).

experiment, such an anomaly was emulated by placing a section of plastic pipe inside the 6 m-long pipe. The thickness of the plastic pipe was 2 mm, while the length was 90 cm. The plastic pipe was positioned at $A - B$ as shown in Fig. 7(b). The outer diameter of the plastic pipe was such that the plastic pipe would be in contact with the inner wall of the steel pipe.

First, measurements were carried out though the feed point $N1$: Fig. 9(a) shows the results. It can be seen that the reflections corresponding to $E1$ and $E2$ are clearly visible, at d_{E1}^{N1} = 0.93 m and d_{E2}^{N1} = 4.74 m, respectively.

Additionally, also two other correlation peaks are clearly visible, at 2.03 m and at 2.80 m. Considering the position of the emulated wall thickening as shown in Fig. 7(b), these correlation peaks correspond to the reflections caused by the beginning (A) and by the end (B) of the wall thickening,

respectively.

The measurement was repeated using $N2$ as feedpoint: the results are shown in Fig. 9(b). Also in this case, there are the correlation peaks at d_{E1}^{N2} = 4.74 m and at d_{E2}^{N2} = 0.96 m caused by reflections at the ends of the pipe. It can also be noticed a peak of the correlation at 1.8 m, which corresponds approximately to the reflection caused at point B.
As for the reflection caused by the wall thickening at A, it is masked by the reflection caused by the end $E2$ at approximately 1 m from $N2$ (opposite with respect to the pipe A-B).

C. Case #3: 6 m-long pipe with 15 cm-long wall thickening

Measurements were repeated by emulating wall-thickening, using a shorter pipe section. Results, not reported here for the sake of brevity, showed that the beginning and the end of the section with wall-thickening were clearly visible until the length of the wall thickening was in the order of 15 cm. The setup configuration is represented in Fig. 7(c).

Figure 10(a) shows the results obtained from measurements at feedpoint $N1$, for a 15-cm long wall thickening. It can be noticed that, in addition to the reflections caused by $E1$ and $E2$, there is another major reflection at 2.22 m. This means that the anomaly caused by the 15 cm-long wall thickening is still clearly visible; in practice, this value represents the achievable spatial resolution, which depends on the pulse width and on the frequency band. The spatial resolution is practically constant along the pipe.

Figure 10(b) shows the results of the correlation obtained, with this same setup configuration, using $N2$ as a feedpoint. Once again, there are the two correlation peaks at d_{E2}^{N2} = 0.93 m and at d_{E1}^{N2} = 4.73 m caused by reflections at the ends of the pipe. Also, a correlation peak at d_{M}^{N2} = 1.61 m can be observed: because of the resolution, the reflections caused by the wall thickening anomaly appear as one single reflection.
The results obtained using $N2$ as feedpoint are consistent with those obtained from $N1$. Indeed, there is a correlation peak at approximately 1.3 m in the configuration of Figure 10(b): there is no intentional anomaly that can be related to this peak; hence, this is a ghost anomaly that can be categorized as a false alarm.

D. Case #4: presence of cuts along the pipe

This test was carried out by making cuts along the pipe to emulate leakage points. This was done in view of a possible adoption of this method for leak localization, also considering the importance of the structural monitoring and investigation [20], [22]–[24]. Two quarter-circular cut ($C1$ and $C2$) were made on the pipe at approximately 2.50 m and 2.75 m from $E1$, as shown in Fig. 7(d).

Figure 11(a) shows the results obtained from measurements at $N1$. The ends $E1$ and $E2$ cause the correlation peaks at d_{E1}^{N1} = 1.09 m and d_{E2}^{N1} = 4.66 m, respectively. Also, it can be seen that there is a slight distortion of the curve at d = 1.35 m which is related to the presence of $C1$. This was also verified through measurements by obstructing the pipe at $C1$,

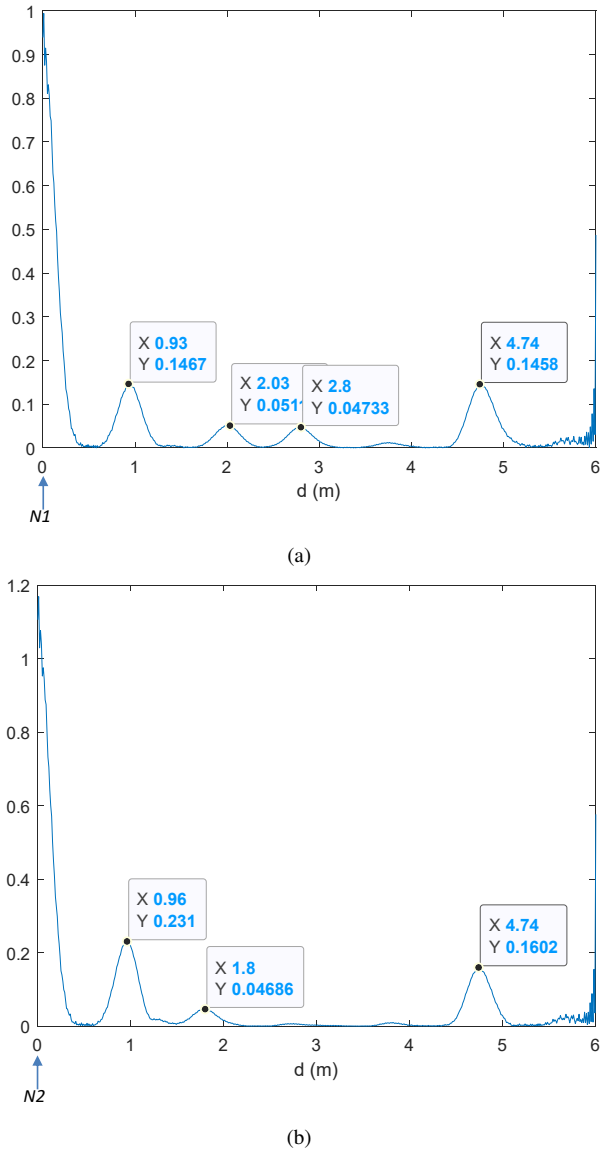

Fig. 9. Measurements on a 6 m-long, in presence of a 90 cm-long wall thickening as schematized in Fig. 7(b). Correlation results obtained through measurements at port $N1$ (a) and at port $N2$ (b).

not reported here for brevity. Finally, there is a correlation peak at d_{C2}^{N1} = 1.65 m which corresponds to the cut $C2$.

Measurements were repeated by connecting to port $N2$. Correlation results are shown in Fig. 11(b). The ends $E1$ and $E2$ lead to the peaks at d_{E1}^{N2} = 4.76 m and d_{E2}^{N2} = 0.93 m, respectively. A reflection at d_{C2}^{N2} = 2.12 m can also be noticed, which is in agreement with the actual position of $C2$ with respect to $N2$.

E. Case #5: Diesel oil

To assess the performance of the system with the pipe carrying lossy liquids, experimental tests were also carried out by filling the 6 m-long pipe with diesel oil.

The quantity k_z was evaluated from (3), considering the frequency-dependent complex permittivity of diesel: this value was assumed equal to the complex permittivity of crude oil,

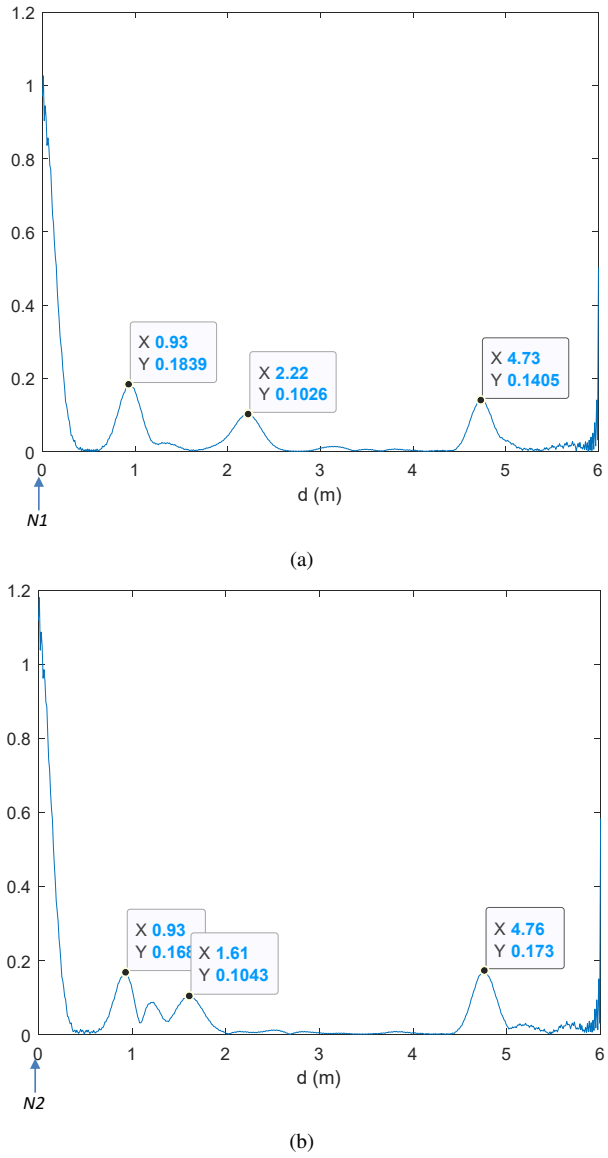

Fig. 10. Measurements on a 6 m-long, in presence of a 15 cm-long wall thickening as schematized in Fig. 7(c). Correlation results obtained through measurements at port $N1$ (a) and at port $N2$ (b).

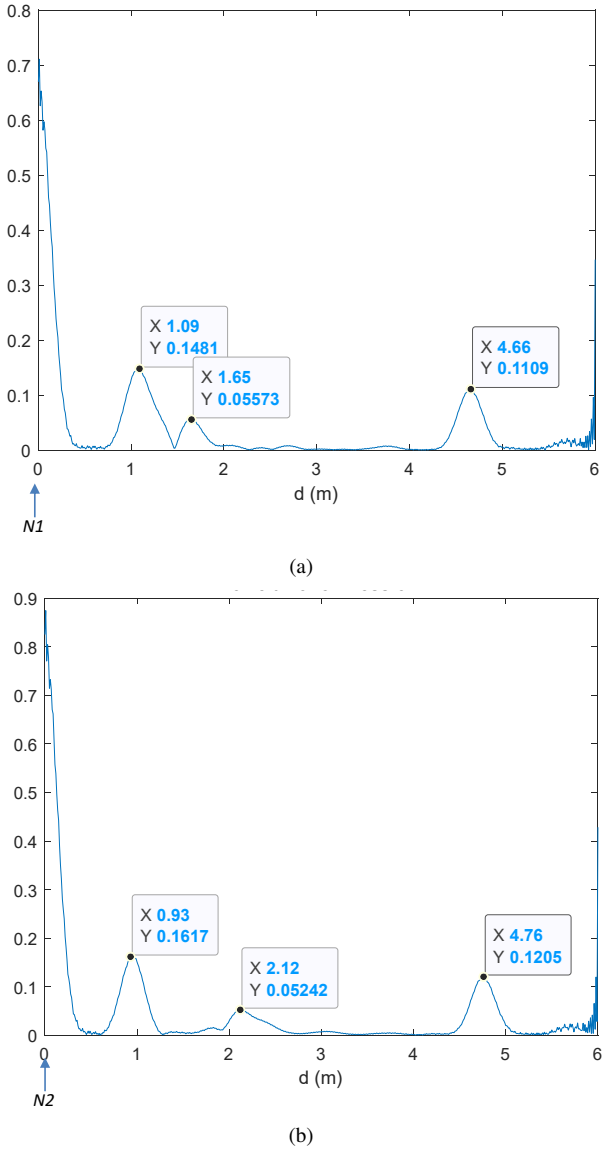

Fig. 11. Measurements on a 6 m-long, in presence of two cuts at $C1$ and $C2$, as schematized in Fig. 7(d). Correlation results obtained through measurements at port $N1$ (a) and at port $N2$ (b)

which is well referenced in the literature [25]. The configuration was as shown in Fig. 7(a). This time, to keep the liquid inside the pipe, two lids were placed at $E1$ and $E2$. To limit the effects of reflections caused by the lids, these were made in PVC.

Figure 12 shows the correlation with the pipe filled with diesel oil, obtained from measurements at the feedpoint $N2$. It can be noticed that there is the reflection caused by $E2$ at d_{E2}^{N2} = 0.95 m, and then a slight reflection at 1.86 m. Nevertheless, because of the strong attenuation caused by the diesel oil, no other reflection appears. This suggests that for lossy liquids, the proposed system presents limitations. On the other hand, the system range is limited by the dynamic range of the instrument, which can be improved adding a power amplifier at the output of the VNA.

V. Discussion of Results and Expected Performance

Table I summarizes the obtained results in terms of estimated position of the anomaly with respect to the (known) reference position. Considering the known positions of the anomalies as conventional true value, it can be noticed that the maximum percentage error is lower than 6 %, except for one false positive. Results demonstrate the suitability of the proposed system and processing strategy for the localization of anomalies along metallic pipes. The proposed system can be used directly on site, by resorting to portable instrumentation, such as hand-held, compact VNAs that are already on the market, and this makes it a viable solution in practical scenarios.

Hence, in view of possible future applications, it is important to discuss the expected performances from a practical perspective and considering non-idealities of the system.

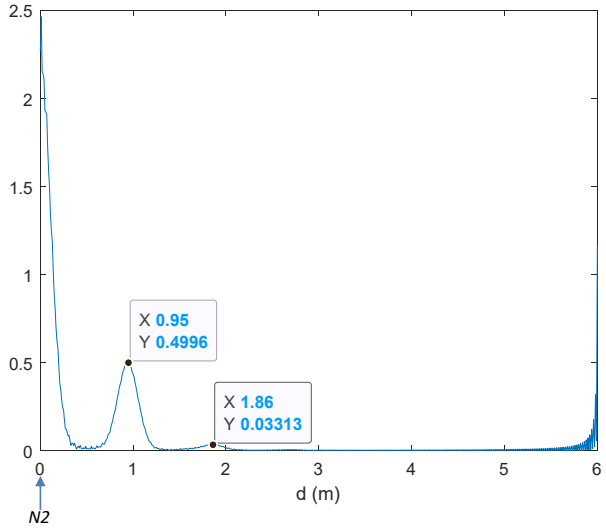

(a)

Fig. 12. Correlation results on diesel oil.

First of all, a numerical analysis was carried out to assess the system performance when the pipe is filled with lossy materials. To this purpose, full-wave simulations were carried out considering a 1 m-long section of pipe, filled with a material with relative dielectric permittivity of 1.3 and loss tangent varying in the range 10^{-3} - 10^{-1}. In the simulations, a pulse in the 2.8-4.0 GHz band was fed at one end, and the magnitude of the transmission coefficient, $S_{21}(f)$, was calculated, thus obtaining the the losses expressed in dB/m. Results are reported in Fig. 13: it can be noticed that the attenuation quickly reaches values that would make the method unsuitable to be applied over long distances. Hence, from a practical point of view, the proposed system may be employed for example for localizing leaks and anomalies in pipes carrying low-loss fluids, such as gases.

On such bases, in practical applications, the proposed system should be implemented as a distributed system: for hundreds-of-meter long pipes, several cross-polarized test points could be included (for example, one test point every 15 or 20 meters). Two consecutive test points could have coverage areas that partially overlap; in this way, the whole pipe length, even hundreds of meters long, could be covered with no interruption.

Another advantageous implementation of the system would be to localize damages or leaks in short pipe sections (such as water lines): in these cases, it is difficult to localize leaks with traditional acoustic methods. On the other hand, by including two coaxial-to-waveguide transitions at the ends of these pipe sections (for example, in correspondence of the valves), the proposed system would allow to detect and localize the presence of anomalies. In such cases, it would also be possible to empty the pipe section, so that the measurement system would not be affected by the liquid losses.

In relation to the practical applications, it should be emphasized that the transverse dimensions of the protrusion of the coaxial-to-waveguide transition are practically negligible with respect to the cross-section of the pipe; therefore, the obstruction to the flow would actually be minimal. However, for the practical implementation of the system, pipes should be manufactured and installed already equipped with the coax to waveguide transition so as to be ready for future inspections.

With regard to insertion losses at the coaxial-to-waveguide transition, from Fig. 2, it has been already observed that the impedance matching at the transition was adequately optimized. Most importantly, because the excitation is Gaussian,

TABLE I
RESULTS OF THE LOCALIZATION OF ANOMALIES

case	description	measured position (m)	reference position (m)
#1	healthy pipe	d_{E1}^{N1}=0.93	d_{E1}^{N1} = 1.00
		d_{E2}^{N1}=4.79	d_{E2}^{N1} = 5.00
		d_{E1}^{N2} = 4.76	d_{E1}^{N2} = 5.00
		d_{E2}^{N2} = 0.93	d_{E2}^{N2} = 1.00
#2	90 cm-long wall thickening	d_{E1}^{N1} = 0.93	d_{E1}^{N1} = 1.00
		d_{E2}^{N1} = 4.74	d_{E2}^{N1} = 5.00
		d_{A}^{N1} = 2.03	d_{A}^{N1} = 2.00
		d_{B}^{N1} = 2.80	d_{B}^{N1} = 2.90
		d_{E1}^{N2} = 4.74	d_{E1}^{N2} = 5.00
		d_{E2}^{N2} = 0.96	d_{E2}^{N2} = 1.00
		d_{A}^{N2} = 1.80	d_{A}^{N2} = 2.00
		d_{B}^{N2}= 0.96*	d_{B}^{N2} = 1.10
#3	15 cm-long wall thickening	d_{E1}^{N1} = 0.93	d_{E1}^{N1} = 1.00
		d_{E2}^{N1} = 4.73	d_{E2}^{N1} = 5.00
		d_{M}^{N1} = 2.22**	d_{M}^{N1} = 2.30
		d_{N}^{N1} = 2.22**	d_{N}^{N1} = 2.45
		d_{E1}^{N2} = 4.76	d_{E1}^{N2} = 5.00
		d_{E2}^{N2} = 0.93	d_{E2}^{N2} = 1.00
		d_{M}^{N2} = 1.61***	d_{M}^{N2} = 1.70
		d_{N}^{N2} = 1.61***	d_{B}^{N2} = 1.55
		d_{l}^{N2} = 1.33	NONE
#4	presence of cuts	d_{E1}^{N1} = 1.09	d_{E1}^{N1} = 1.10
		d_{E2}^{N1} = 4.66	d_{E2}^{N1} = 4.90
		d_{C1}^{N1} = 1.35**	d_{C1}^{N1} = 1.40
		d_{C2}^{N1} = 1.65	d_{C2}^{N1} = 1.65
		d_{E1}^{N2} = 4.76	d_{E1}^{N2} = 5.00
		d_{E2}^{N2} = 0.93	d_{E2}^{N2} = 1.00
		d_{C1}^{N2} = NA	d_{C1}^{N2} = 2.50
		d_{C2}^{N2} = 2.12	d_{C2}^{N2} = 2.25
#5	diesel oil	d_{E1}^{N1} = 0.99	d_{E1}^{N1} = 1.00
		d_{E2}^{N1} = NA	d_{E2}^{N1} = 5.00
		d_{E1}^{N2} = NA	d_{E1}^{N2} = 5.00
		d_{E2}^{N2} = 0.95	d_{E2}^{N2} = 1.00

*covered by the reflection at 0.96 caused by $E2$
*the 15 cm-long anomaly falls under the same peak (resolution limit
**the 15 cm-long anomaly falls under the same peak (resolution limit)

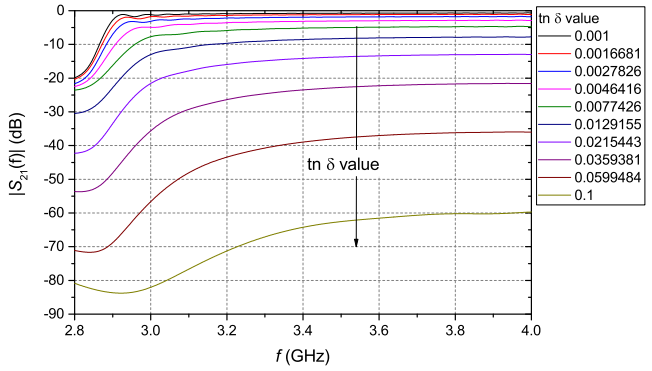

Fig. 13. Simulation results on a 1 m-long pipe section: $S_{21}(f)$ curves for different values of loss tangent.

the spectrum of the signal is also Gaussian; it follows that most of the energy is concentrated in the central portion of the frequency range of interest, where the matching is better than -10 dB. These results show that reflection losses at the coaxial-to-waveguide transition are not a limiting factor for the practical implementation of the system.

Finally, to assess the influence of the conductor losses, full-wave simulations were carried out considering a pipe made of a perfect conductor and a piper made of stainless steel (considering an electrical conductivity of 1.4×10^6 S/m). Results, not reported here for the sake of brevity, showed that dispersion is entirely due to the dispersiveness of the TE11 mode; hence, neglecting conductor losses does not represent a limiting aspect for the evaluation of correlation.

VI. Conclusions

In this work, an innovative system for structural health monitoring of metallic pipes was presented. The proposed system relies on exploiting the pipeline as a circular waveguide for the propagation of an EM signal.

In the proposed system, the EM test signal is injected in the pipeline/waveguide through a coaxial/waveguide transition that is made on the surface of the pipe (rather than on the cross section of the pipe, as reported in the literature related to this application scenario).

A dedicated processing strategy was developed to improve the localization of anomalies along the pipe: this strategy was based on the correlation of the measured reflected signal and the ideal reflected signal created in Matlab.

Finally, an operating strategy that consists in placing two coaxial-to-waveguide transition connectors (at a distance from each other) and serving as two independent test-points was proposed for practical purposes. In practical applications, when an anomaly is detected from the measurement at one port, a separate measurement at the second port can be used as counter-check on the position of the reflection/anomaly.

To verify the suitability of the proposed system and processing strategy, several experiments were carried out on a 6 m-long pipe with different anomalies. Results showed that the proposed system can successfully localize the position of the anomalies. Further work will be dedicated to experiment the proposed method in different conditions (namely longer pipes, pipes with different diameters and pipes with different defects, pipes carrying lossy liquids, etc.) This will require a systematic, extensive analysis of a number of anomalies and defects, representative of practical case scenarios, also in presence of liquids.

Acknowledgment

This work was supported in part by the Italian Ministry of Education and Research (MIUR) under the *Proof of concept* initiative, through the research project "SMARTER-Systems and Monitoring Apparata based on Reflectometric Techniques for Enhanced Revealing" (project number: POC01_00118) and in part by the Italian Ministry of Education and Research (MIUR) under the initiative 'Departments of Excellence' (Italian Law no. 232/2016), through the project titled 'ICT for Health' at the Department of Information Technology and Electrical Engineering of the University of Naples Federico II.

References

[1] L. Boaz, S. Kaijage, and R. Sinde, "An overview of pipeline leak detection and location systems," in *Proceedings of the 2nd Pan African International Conference on Science, Computing and Telecommunications (PACT 2014)*, pp. 133–137, July 2014.

[2] R. Cramer, D. Shaw, R. Tulalian, P. Angelo, and M. van Stuijvenberg, "Detecting and correcting pipeline leaks before they become a big problem," *Marine Technology Society Journal*, vol. 49, no. 1, pp. 31–46, 2015.

[3] I. Baran, I. Lyasota, and K. Skrok, "Acoustic emission testing of underground pipelines of crude oil of fuel storage depots.," *Journal of Acoustic Emission*, vol. 33, 2016.

[4] G. M. Light, S. Y. Kim, R. L. Spinks, H. Kwun, and P. C. Porter, "Monitoring technology for early detection of internal corrosion for pipeline integrity," tech. rep., Southwest Research Institute (US), 2003.

[5] R. Munser, M. Roßner, M. Hartrumpf, and H. Kuntze, "Microwave backscattering sensor for the detection of hidden material inhomogeneities eg pipe leakages," in *Proceedings of the 9th International Trade Fair and Conference for Sensors, Transducers & Systems, Nürnberg*, pp. 275–280, 1999.

[6] M. S. Higgins and P. O. Paulson, "Fiber optic sensors for acoustic monitoring of pccp," in *Pipelines 2006: Service to the Owner*, pp. 1–8, 2006.

[7] Z. Liu and Y. Kleiner, "State-of-the-art review of technologies for pipe structural health monitoring," *IEEE Sensors Journal*, vol. 12, pp. 1987–1992, June 2012.

[8] D. W. Greve, I. J. Oppenheim, A. P. Wright, and W. Wu, "Design and testing of a mems acoustic emission sensor system," in *Sensors and Smart Structures Technologies for Civil, Mechanical, and Aerospace Systems 2008*, vol. 6932, p. 69321P, International Society for Optics and Photonics, 2008.

[9] V. Giurgiutiu and C. Soutis, "Guided wave methods for structural health monitoring," *Encyclopedia of aerospace engineering*, 2010.

[10] S. Mariani, S. Heinlein, and P. Cawley, "Location specific temperature compensation of guided wave signals in structural health monitoring," *IEEE Transactions on Ultrasonics, Ferroelectrics, and Frequency Control*, pp. 1–1, 2019.

[11] R. Soman, P. Kudela, K. Balasubramaniam, S. Singh, and P. Malinowski, "A study of sensor placement optimization problem for guided wave-based damage detection," *Sensors (Switzerland)*, vol. 19, no. 8, 2019.

[12] B. Vogelaar, G. Priems, K. Bourgonje, and M. Golombok, "Time-lapse acoustic monitoring of deteriorating pipes," *Structural Health Monitoring*, vol. 18, no. 5-6, pp. 1995–2003, 2019.

[13] G. M. D'Aucelli, N. Giaquinto, C. Guarnieri Caló Carducci, M. Spadavecchia, and A. Trotta, "Uncertainty evaluation of the unified method for thermo-electric module characterization," *Measurement*, vol. 131, pp. 751 – 763, 2019.

[14] W. Alobaidi and E. Sandgren, "Detection of defects in spiral/helical pipes using rf technology," in *11th Pipeline Technology Conference*, pp. 22–33, 2016.

[15] L. Liu and Y. Ju, "A high-efficiency nondestructive method for remote detection and quantitative evaluation of pipe wall thinning using microwaves," *NDT & E International*, vol. 44, no. 1, pp. 106 – 110, 2011.
[16] L. Liu, "Application of microwave for remote ndt and distinction of biofouling and wall thinning defects inside a metal pipe," *Journal of Nondestructive Evaluation*, vol. 34, no. 4, pp. 1–8, 2015.
[17] K. Abbasi and H. Hashizume, "Microwave detection of circumferential crack in piping system of nuclear power plants," in *Proc. 2nd Int. Conf. Technical Inspection NDT*, Citeseer, 2008.
[18] L. Angrisani, G. Cannazza, A. Cataldo, E. De Benedetto, and E. Piuzzi, "A new microwave method for on-site integrity monitoring of pipelines," in *2020 IEEE International Instrumentation and Measurement Technology Conference (I2MTC)*, pp. 1–6, 2020.
[19] A. Cataldo, E. De Benedetto, G. Cannazza, A. Masciullo, N. Giaquinto, G. D'Aucelli, N. Costantino, A. De Leo, and M. Miraglia, "Recent advances in the tdr-based leak detection system for pipeline inspection," *Measurement: Journal of the International Measurement Confederation*, vol. 98, pp. 347–354, 2017.
[20] A. Cataldo, E. De Benedetto, G. Cannazza, E. Piuzzi, and E. Pittella, "TDR-based measurements of water content in construction materials for in-the-field use and calibration," *IEEE Transactions on Instrumentation and Measurement*, vol. 67, pp. 1230–1237, May 2018.
[21] D. M. Pozar, *Microwave engineering*. Hoboken, NJ: John Wiley & Sons, 4 ed., 2009.
[22] A. Cataldo, E. De Benedetto, G. Cannazza, E. Piuzzi, and N. Giaquinto, "Embedded TDR wire-like sensing elements for monitoring applications," *Measurement*, vol. 68, pp. 236–245, 2015.
[23] A. Cataldo, E. De Benedetto, G. Cannazza, A. Masciullo, N. Giaquinto, G. D'Aucelli, N. Costantino, A. De Leo, and M. Miraglia, "Recent advances in the TDR-based leak detection system for pipeline inspection," *Measurement*, vol. 98, pp. 347–354, 2017.
[24] N. Giaquinto, G. D'Aucelli, E. De Benedetto, G. Cannazza, A. Cataldo, E. Piuzzi, and A. Masciullo, "Criteria for automated estimation of time of flight in TDR analysis," *IEEE Transactions on Instrumentation and Measurement*, vol. 65, no. 5, pp. 1215–1224, 2016.
[25] K. Folgero, "Broad-band dielectric spectroscopy of low-permittivity fluids using one measurement cell," *IEEE Transactions on Instrumentation and Measurement*, vol. 47, no. 4, pp. 881–885, 1998.

Andrea Cataldo (M'12, SM'13) received the M.S. degree in materials engineering and the Ph.D. degree in information engineering from the University of Salento, Lecce, Italy, in 1998 and 2003, respectively.
From 2000 to 2004, he was with the University of Lecce, where he worked on research projects in the field of characterization of optoelectronic devices, telecommunication applications, and microwave measurements. Since January 2005, he has been a Researcher with the Department of Engineering for Innovation, University of Salento, Lecce, where he is currently an Associate Professor of electric and electronic measurements. He has coauthored more than 150 publications.
Prof. Cataldo is also the co-founder of a spin-off company of the University of Salento, namely MoniTech S.r.l.
His research interests include reflectometry and microwave measurement techniques, uncertainty evaluation, and characterization and optimization of sensors.
Prof. Cataldo is a member the IEEE I&M Society and of the Italian Group of Electrical and Electronic Measurements (GMEE).

Egidio De Benedetto (M'14, SM'16) received the M.S. degree in materials engineering and the Ph.D. degree in information engineering from the University of Salento, Lecce, Italy, in 2006 and 2010, respectively. He has been with the Institute of Microelectronics and Microsystems, National Research Council, Naples, Italy, from 2010 to 2012.
Since 2012 through 2019, he has been a Research Fellow with the Department of Engineering for Innovation, University of Salento. Since 2019, Egidio De Benedetto is an Associate Professor with the Department of Electrical Engineering and Information Technology of the University of Naples Federico II, Naples, Italy.
His current research interests include the dielectric characterization of materials, microwave reflectometry systems for monitoring applications, and measurements for augmented reality systems.

Leopoldo Angrisani (F'19) is a Full Professor of electrical and electronic measurements with the Department of Information Technology and Electrical Engineering, University of Naples Federico II, Naples, Italy. He is also the General Manager and the Director of the Center of Advanced Measurement and Technology Services (CeSMA), Naples, and a member of the Board of the Ph.D. Program in information technology and electrical engineering with the University of Naples Federico II.
Prof. Angrisani is involved in several industrial research projects (also in cooperation with small, medium, and large enterprises), for which he has been scientific coordinator. He is currently involved in designing and developing the strategic pillars on which the national Competence Center on Industry 4.0, MedITech, led by Federico II University, Naples, Italy.
He has authored or coauthored more than 300 scientific articles, one-third of which are published in relevant international journals with impact factor. His current research interests include communication systems and networks test and measurement, measurements for Internet of Things applications, compressive sampling-based measurements, measurements for industry 4.0, and measurement uncertainty.
Prof. Angrisani is a Fellow Member of the IEEE Instrumentation and Measurement and Communications Societies, the Chair of the IEEE Instrumentation and Measurement Society Italy Chapter, the Honorary Chairman of the first edition (M&N 2019) of the IEEE International Symposium on Measurements and Networking 2019, and the General Chairman of the second edition (MetroInd4.0&IoT 2019) of the IEEE International Workshop on Metrology for Industry 4.0 and IoT 2019.

Giuseppe Cannazza received the Laurea degree in physics from the University of Salento (Lecce, Italy) in 2000 and the M.S. degree in material science and technology from the University of Pavia (Pavia, Italy), in 2003. In 2001, he was a Researcher with an international consulting company, where he worked in the environmental field. From 2003 to 2004, he was a Technical Advisor with a German company, where he worked on the development of an innovative measurement method for water content sensing in materials through low-resolution inside-out nuclear magnetic resonance. Since 2007, he has been with the Department of Engineering for Innovation of the University of Salento, where he is currently a Research Fellow. His research interests include reflectometry and microwave measurement techniques, uncertainty evaluation, and characterization and optimization of sensors for industrial applications.

Emanule Piuzzi (M'09) Emanuele Piuzzi (M'09) received the M.S. (cum laude) and Ph.D. degrees in electronic engineering from the Sapienza University of Rome, Rome, Italy, in 1997 and 2001, respectively. He is currently an Associate Professor of Electrical and Electronic Measurements with the Department of Information Engineering, Electronics and Telecommunications, Sapienza University of Rome. His research activities include the measurement of complex permittivity of materials, time domain reflectometry applications, and biomedical instrumentation design.